Insights into interferon regulatory factor activation from the crystal structure of dimeric IRF5

Weijun Chen, Suvana S. Lam, Hema Srinath, Zhaozhao Jiang, John J. Correia, Celia A. Schiffer, Katherine A. Fitzgerald, Kai Lin and William E. Royer, Jr.

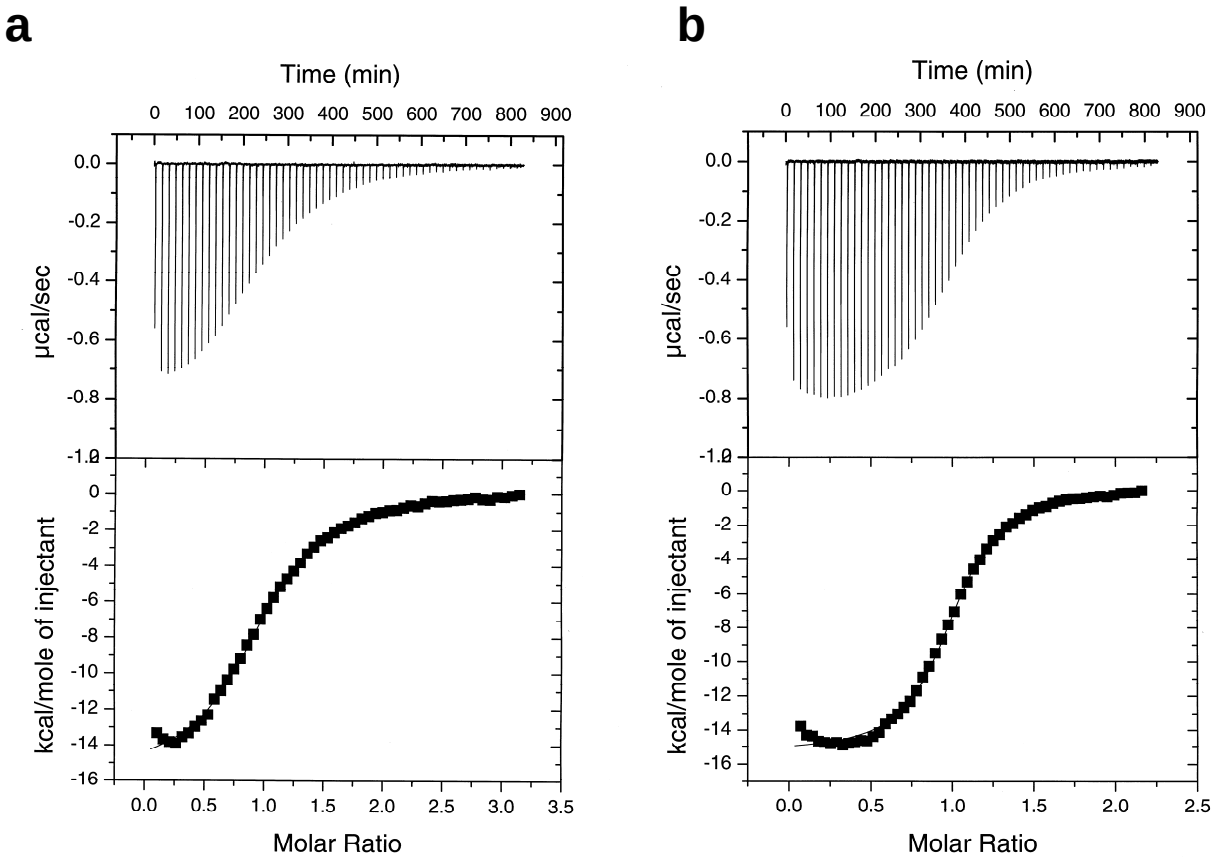

Supplementary Figure 1 ITC traces for the binding of CBP to (**a**) IRF5 (222-467) and (**b**) IRF5 (222-467) S430D. The steeper slope observed in (**b**) reflects the tighter binding of CBP to IRF5 S430D compared with IRF5. The thermodynamic binding parameters are provided in Table 1.

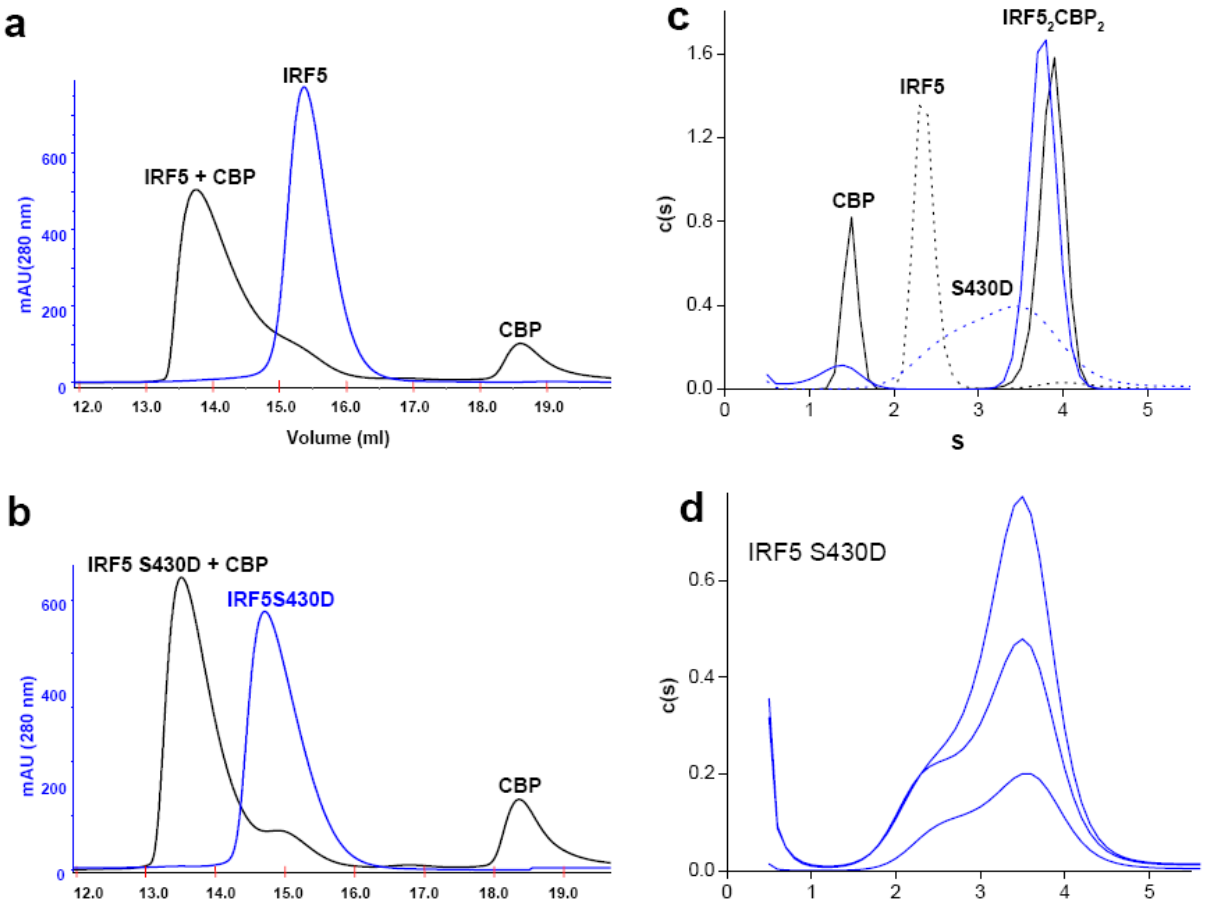

Supplementary Figure 2 Gel exclusion chromatography and sedimentation velocity on IRF5 (222-467) and IRF5 (222-467) S430D. (**a**) Comparison of IRF5 by gel exclusion chromatography at a loading concentration of 200μM in the presence and absence of CBP (2067-2112). In the absence of CBP (blue) the elution peak corresponds to an apparent mass of 37 kDa, consistent with IRF5 running as a monomer. (IRF5 (222-467) is 30 kDa.). In the presence of CBP (black), the elution peak shifts by 1.5ml to a value corresponding to an apparent molecular mass of 87 kDa, which likely represents a complex formed from two IRF5 molecules and two CBP molecules. (**b**) IRF5 S430D at a loading concentration of 180μM in the presence and absence of CBP. The elution of IRF5S430D is consistent with a slightly higher molecular mass from that of wild-type IRF5, suggesting reversible association. Elution in the presence of CBP is consistent with a complex formed from two IRF5 molecules and two CBP molecules as in wild-type. (**c**) Sedfit distribution plots c(s) show analysis of data for IRF5 (black) and a phosphomimic of IRF5 S430D (blue), alone (dotted lines) and in the presence of excess CBP (solid lines) in sedimentation velocity runs. IRF5 runs at a monomer at this concentration (6.7 μM) with 4-6% dimer. S430D runs as a mixture of monomer and stable dimer at this concentration (9.5 μM) but with > 50% of the material in dimer form. CBP causes a shift of all species to faster zones consistent with the formation of a 2:2 complex running at 3.93 $s_{20,w}$ for IRF5 and 3.89 $s_{20,w}$ for S430D. The excess CBP is evident as slow zones near 1.5 s. (**d**) Sedfit distribution plots c(s) of IRF5 S430D at 4.2, 9.8 and 13.9 μM.

The patterns are all bimodal and reflect a mixture of monomer and stable dimer forms. Normalization of DCDT+2 g(s) distributions (see supplementary Fig. 3) reveals no significant redistribution of these species during the experiments. In spite of this slow equilibrium, CBP is able to recruit all species into a 2:2 complex (**c**).

Analytical Ultracentrifugation Methods. Sedimentation velocity was performed at 19.7^{o}C and 50 K in SEDVEL60K centerpiece by simply dilution of the stock IRF5 samples into dialysis buffer (20 mM HEPES, 0.1 mM EDTA, 100 mM NaCl at pH 7.3) in the presence and absence of 2 mM TCEP. Data were also collected on CBP/IRF5 ratios with an excess of CBP. All data were collected at 280 nm (1 average, 0.002 cm spacing) and analyzed by DCDT^{+} [2] and Sedfit [3] to estimate weight average S values and to generate g(s) and c(s) plots. At low protein concentration (< 10 uM) IRF5 alone sediments with concentration independence ($S_{20,w}$ = 2.36 +/- 0.02) and fitting with Sedanal [4] reveals the presence of predominantly monomeric IRF5 with a small amount of irreversible dimer (4–6% with or without TCEP). Addition of CBP causes a significant shift of the IRF5 zone to $S_{20,w}$ = 3.93 +/- 0.02. This shift occurs as an all or none transition and reflects a tight interaction between IRF5 dimer and CBP. Fitting with Sedanal is consistent with this being an $IRF5_2CBP_2$ complex. Runs were also performed on a phosphomimic S430D of IRF5. Alone and in the presence of 2 mM TCEP it runs as a mixture of monomer (or weak monomer-dimer) and stable dimer. This suggests a conformational change that crosslinks and stabilizes the dimer. Upon the addition of excess CBP a stable $S430D_2CBP_2$ complex is formed that runs at $S_{20,w}$ = 3.89 +/- 0.04.

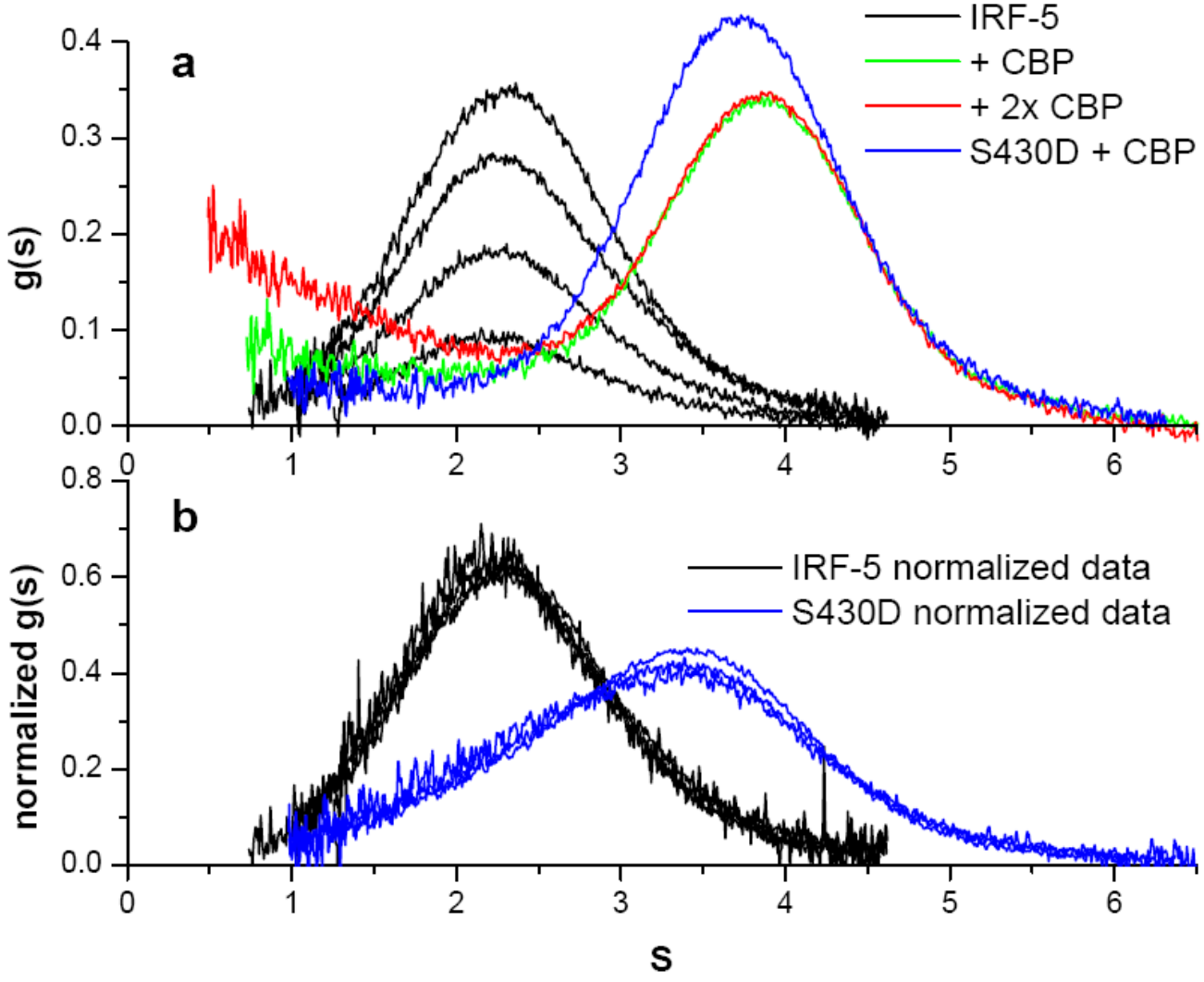

Supplementary Figure 3. **(a)** Sedimentation coefficient distributions g(s) for IRF5 with and without excess CBP. The IRF5 data is concentration independent (< 10 μM) as shown by the normalized g(s) plot in panel b. Addition of excess CBP shifts the peak consistent with tight complex formation; notice the superposition of the complex peak at two CBP concentrations. The excess CBP is seen as a trailing zone in the g(s) plots but appears as a peak in a c(s) plot (see Figure 1c). **(b)** Normalized g(s) distributions for IRF5 WT and S430D. At low concentrations (< 10 μM) IRF5 is a monomer. Over this same concentration range (See Fig. 1d) S430D runs as a mixture of monomer and stable dimer. These stable dimers are not influenced by the addition of 2 mM TCEP. Addition of CBP to S430D also causes a shift of both species to a stable complex (panel **a** and Supplementary Fig. 2c).

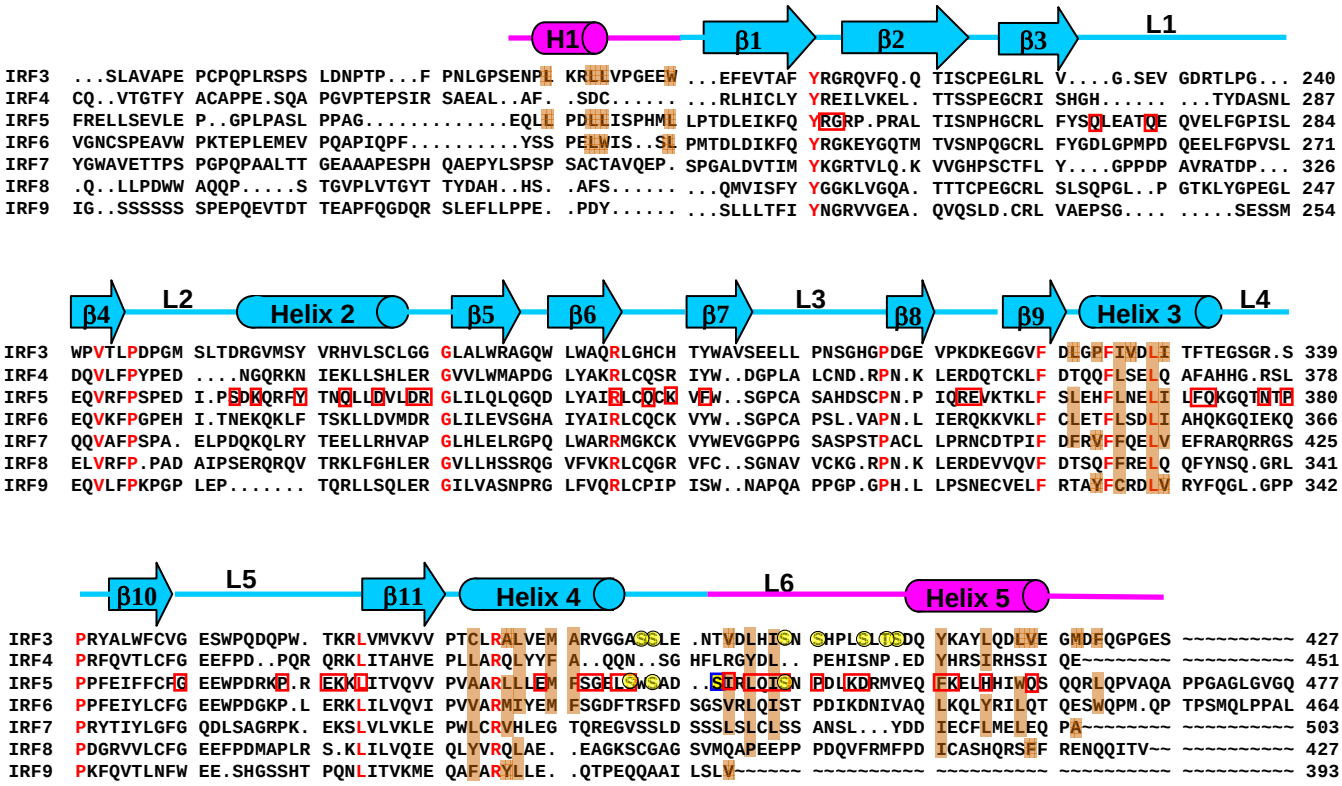

Supplementary Figure 4 Sequence alignment of the C-terminal transactivation domains of human IRF members that contain the interferon association domain (IAD). Shown above the sequence alignment is the secondary structure based on the IRF5 crystal structure, with the IAD in cyan and the autoinhibitory regions in magenta. Identical residues in IRF3 – IRF9 are shown in red. Hydrophobic residues within the helices 1, 3 and 4 and in the C-terminal autoinhibitory domain, as identified in the structure of monomeric IRF3 are highlighted in brown. Putative phorphorylation sites for IRF3 and IRF5 are shown in yellow circles, with the mutated Ser 430 shown also highlighted in yellow but outlined in a blue rectangle. Residues involved in the dimeric interface of IRF5 are outlined in red rectangles. (Modified from Qin et al. [1].)

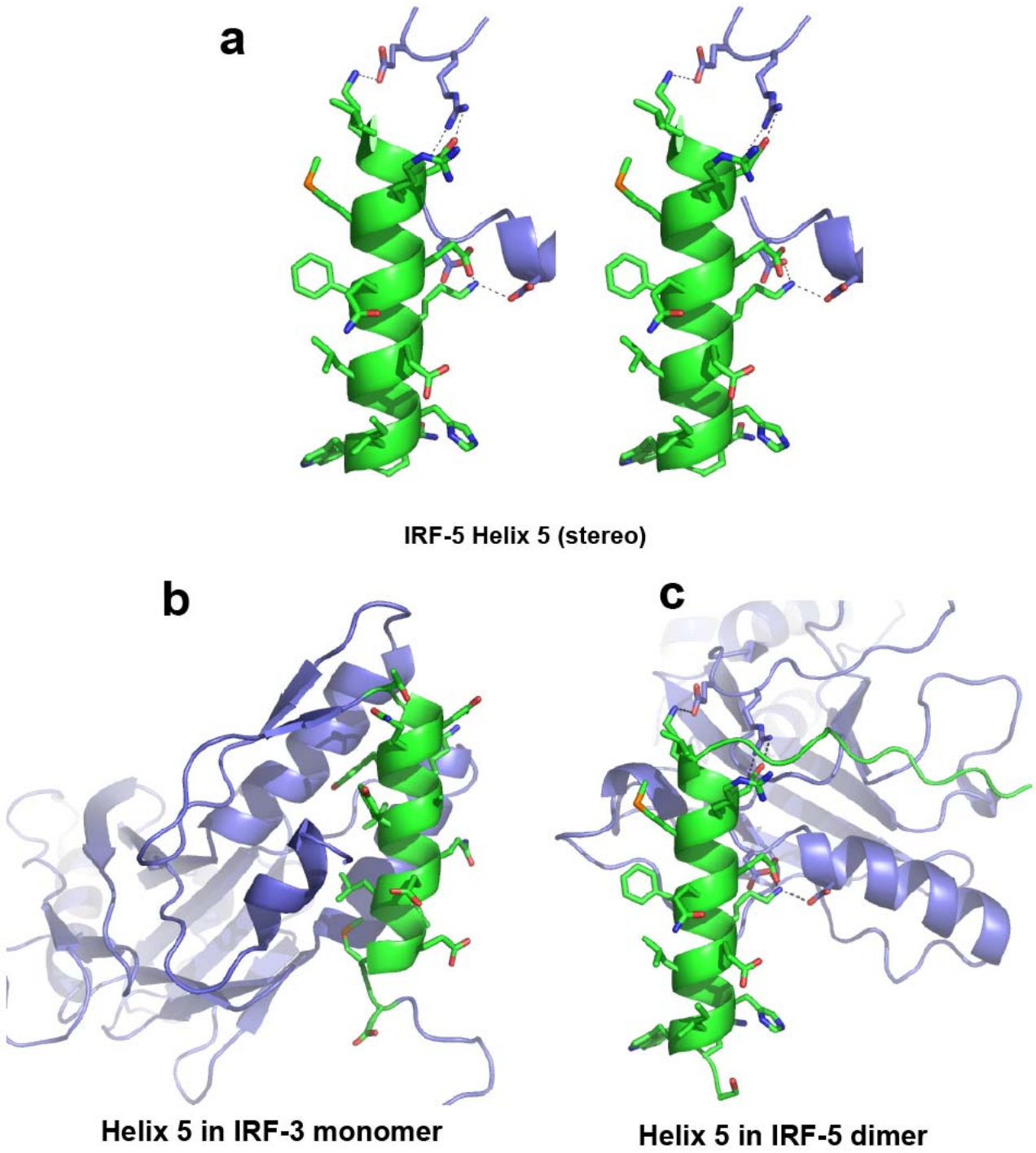

Supplementary Figure 5. Amphipathic nature of helix 5. (**a**) Stereodiagram of helix 5 (green) in IRF5 dimer. Note the largely hydrophobic residues on the left side and mainly hydrophilic residues on the right side of the helix, properties shared by IRF5 and IRF3. (**b**) Helix 5 in IRF3 monomer. The largely hydrophobic side of helix 5 is involved in extensive intramolecular contacts with the CBP/p300 binding surface of IRF3. (**c**) Helix 5 in the IRF5 dimer. Dimeric contacts primarily involve hydrophilic regions of helix 5. The similar hydrophobic surface evident on the left side of helix 5 in IRF5 strongly suggests that it will also mask the CBP/p300 binding surface in the autoinhibited monomer of IRF5.

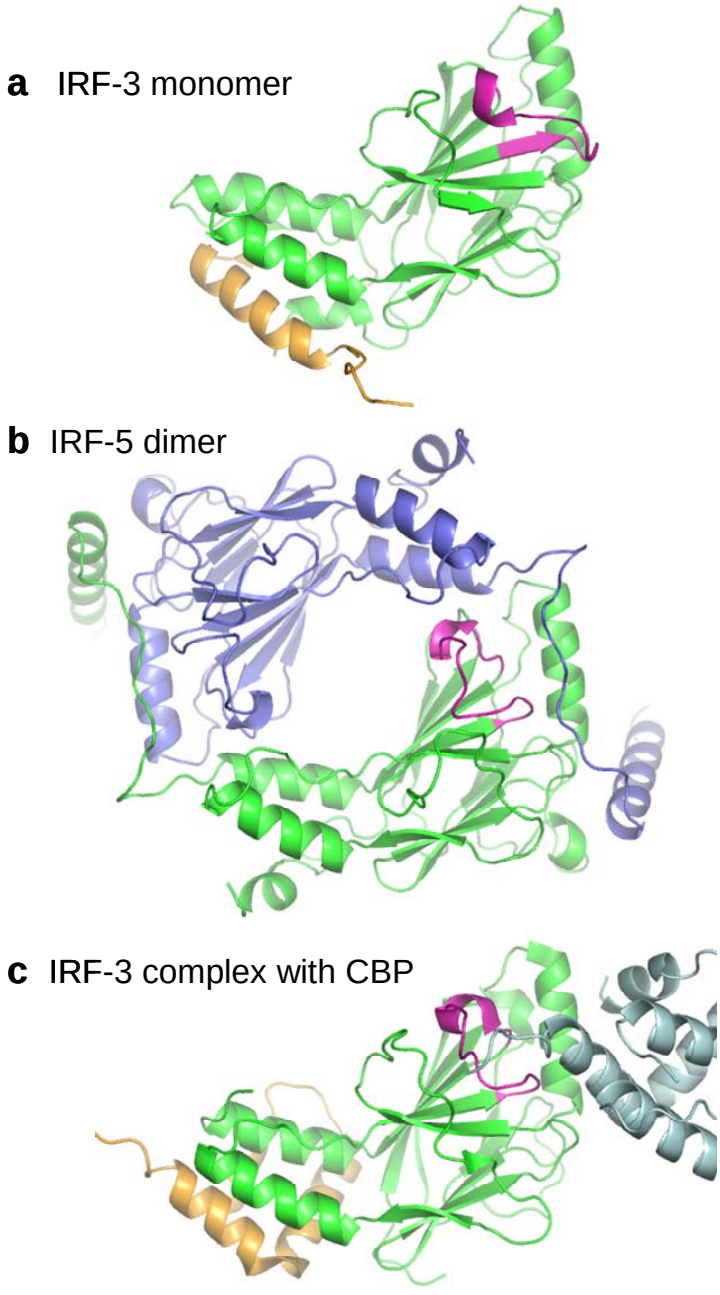

Supplementary Figure 6 Crystal structures of IRF3 and IRF5 show plasticity of Loop L5 (magenta). (**a**) Ribbon diagram of the IRF3 monomer with loop L5 (including C-terminus of β10) in magenta and the C-terminal autoinhibitory region in gold. (**b**) Ribbon diagram of the IRF5 dimer, showing the different conformation of loop L5 relative to that in the autoinhibited IRF3, which is required to avoid steric clashes with the partner subunit. (**c**) Ribbon diagram of the structure of IRF3 in complex with CBP (gold). A lattice contact with another CBP-IRF3 complex (light blue) is coupled with a conformational change in the L5 loop relative to that observed in the autoinhibited IRF5 structure (**a**). This implies a substantial plasticity of Loop L5 that would allow IRF3 to form a dimer similar to that observed for IRF5 (**b**). (Superposition of 14 loop L5 α-carbons between IRF5 and IRF3/CBP results in an rms deviation of 1.3Å, in contrast to rms deviations of 3.4 and 3.8Å for the equivalent superposition of monomeric IRF3 with IRF5 and the IRF3/CBP complex, respectively.)

Supplementary References

1. Qin, B.Y. et al. Crystal structure of IRF3 reveals mechanism of autoinhibition and virus-induced phosphoactivation. *Nat Struct Biol* **10**, 913-21 (2003).
2. Philo, J.S. Improved methods for fitting sedimentation coefficient distributions derived by time-derivative techniques. *Anal Biochem* **354**, 238-46 (2006).
3. Schuck, P., Perugini, M.A., Gonzales, N.R., Howlett, G.J. & Schubert, D. Size-distribution analysis of proteins by analytical ultracentrifugation: strategies and application to model systems. *Biophys J* **82**, 1096-111 (2002).
4. Stafford, W.F. & Sherwood, P.J. Analysis of heterologous interacting systems by sedimentation velocity: curve fitting algorithms for estimation of sedimentation coefficients, equilibrium and kinetic constants. *Biophys Chem* **108**, 231-43 (2004).